NASA TECHNICAL NOTE

NASA TN D-4574

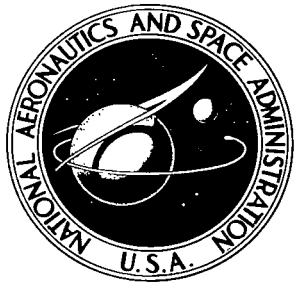

A SUMMARY OF ROTOR-HUB BENDING MOMENTS ENCOUNTERED BY A HIGH-PERFORMANCE HINGELESS-ROTOR HELICOPTER DURING NAP-OF-THE-EARTH MANEUVERS

by William J. Snyder

Langley Research Center
Langley Station, Hampton, Va.

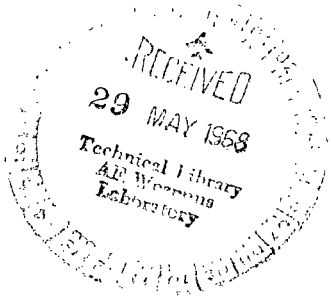

NATIONAL AERONAUTICS AND SPACE ADMINISTRATION • WASHINGTON, D. C. • MAY 1968

NASA TN D-4574

A SUMMARY OF ROTOR-HUB BENDING MOMENTS ENCOUNTERED BY A HIGH-PERFORMANCE HINGELESS-ROTOR HELICOPTER DURING NAP-OF-THE-EARTH MANEUVERS

By William J. Snyder

Langley Research Center
Langley Station, Hampton, Va.

NATIONAL AERONAUTICS AND SPACE ADMINISTRATION

For sale by the Clearinghouse for Federal Scientific and Technical Information
Springfield, Virginia 22151 – CFSTI price $3.00

A SUMMARY OF ROTOR-HUB BENDING MOMENTS ENCOUNTERED BY A HIGH-PERFORMANCE HINGELESS-ROTOR HELICOPTER DURING NAP-OF-THE-EARTH MANEUVERS

By William J. Snyder
Langley Research Center

SUMMARY

A brief investigation was recently undertaken at Langley Research Center to study the flying qualities and structural loads of a hingeless-rotor helicopter, the XH-51N, during nap-of-the-earth maneuvers. This investigation was part of Langley's continuing flight research with hingeless-rotor helicopters.

The series of nap-of-the-earth maneuvers was devised primarily to simulate military helicopter operation in a hostile environment where remaining undetected is a necessity. Most of the maneuvers employed are abrupt turns, starts, and stops which require a helicopter with very good maneuverability to perform them effectively. Previous investigations have shown that the cyclic loads of the hingeless rotor can be very high during these abrupt types of maneuvers.

Time histories of the rotor-hub bending moments measured during the investigation show that during the abrupt maneuvers a rapid buildup in the cyclic bending moments occurs. This buildup, in most cases, exceeds the assigned endurance limit of the rotor hub to such an extent that the service life of the hub is significantly shortened. These results indicate that any operational hingeless-rotor helicopter utilized for nap-of-the-earth flying must be carefully evaluated with respect to the service life of the rotor system.

INTRODUCTION

The helicopter, through its unique capabilities, lends itself handily to military operation over unfamiliar terrain or in areas inaccessible to fixed-wing aircraft and ground vehicles. It can fly at low levels and follow the terrain by abruptly maneuvering to avoid obstructions. It can also rise quickly to an altitude for observation purposes and return quickly to cover to avoid detection. These tasks, which are accomplished by nap-of-the-earth maneuvers, demand the fullest utilization of the helicopter and require high maneuverability. The improved control-response characteristics of the hingeless-rotor

helicopters, as reported in references 1 and 2, should make them effective aircraft for nap-of-the-earth flying, but an investigation of the rotor dynamic loads is necessary to determine to what extent they warrant concern.

The current hingeless-rotor flight research, utilizing the XH-51N, is a follow-on to wind-tunnel tests of hingeless-rotor models in the Langley full-scale tunnel and the Langley transonic dynamics tunnel and to preliminary flight research with a rudimentary hingeless-rotor helicopter, XH-13N (OH-13G). (See refs. 1, 2, and 3.) It was discovered that an undesirable buildup in the cyclic chordwise moments occurred during maneuvers with the XH-13N (ref. 3).

The present paper summarizes some of the rotor-hub bending moments encountered during a brief flight investigation of the flying qualities and dynamic loads characteristics of a high-performance hingeless-rotor helicopter during nap-of-the-earth maneuvers. The rotor structural loads, which are of most concern during abrupt maneuvering, are presented to indicate how they may restrict the maneuver capability of current hingeless-rotor helicopters and how they may influence the design of future hingeless-rotor helicopters. Some of the problem areas which arose during this investigation are discussed qualitatively in appendix A.

SYMBOLS

A_1 lateral cyclic blade pitch angle (cyclic pitch for primarily lateral control moments), positive for blade leading edge up at $\psi = 180^{\circ}$, radians

B_1 longitudinal cyclic blade pitch angle (cyclic pitch for primarily longitudinal control moments), positive for blade leading edge up at $\psi = 270^{\circ}$, radians

p helicopter rolling velocity, positive for right roll, radians per second

q helicopter pitching velocity, positive for nose-up pitching, radians per second

θ instantaneous blade-section pitch angle, angle between line of zero lift of blade section and plane perpendicular to rotor shaft, radians or degrees

θ_0 collective pitch angle at blade root, radians or degrees

θ_1 resultant amplitude of first-harmonic cyclic pitch angle $\sqrt{A_1^2 + B_1^2}$, radians or degrees

ψ blade azimuth angle measured from downwind position in direction of rotor rotation, degrees

VEHICLE AND INSTRUMENTATION

The vehicle utilized in the present investigation is the hingeless-rotor helicopter, XH-51N, shown in figure 1. The basic configuration is a three-blade single-rotor helicopter with cantilevered flexible blades. It is fairly clean aerodynamically, with retractable gear and with fairings around the mast area. The XH-51N is unique in the way in which the control system incorporates a free gyro. The gyro, seen in figure 2, precesses to provide feathering inputs to blades when subjected to an applied moment provided by the pilot through a system of springs, as shown in figure 3 (from ref. 4). The gyro is also subject to feedback from the flapwise and chordwise blade moments (ref. 5). The major physical parameters of the XH-51N are shown in table I.

The extensive handling-qualities and structural-loads instrumentation of the XH-51N is listed in appendix B. While most of the instrumentation was monitored during the data reduction for this investigation, the structural loads relating to the rotor hub at station 6 (fig. 2) were found to be of most concern and are indicative of the severity of the maneuvers; therefore, structural data will be presented only for the rotor-hub flapwise and chordwise bending at station 6 (6 in. or 15.2 cm from center line of main rotor).

The data were recorded on two onboard 36-channel oscillographs. In addition to the onboard recording equipment, four channels of structural data were transmitted by telemetry to a direct readout oscillograph on the ground for constant monitoring.

TASK

The maneuvers selected are, for the most part, variations of the "Army Dozen" (ref. 6). The maneuvers utilized for this flight investigation were:

Slalom course

Teardrop turn

S-turn

Hit-the-deck

Scramble

Whoa-boy

Only one pilot was involved in the maneuvers, each of which was performed several times for both practice and data.

Slalom Course

The slalom course as illustrated in figure 4(a) is a series of rapid roll reversals through a line of pylons or markers. This maneuver was devised to simulate a combat task of terrain following or evasive action.

The slalom maneuvers were performed with the markers spaced at distances of either 200 feet or 400 feet (61 m or 122 m). The maneuvers were performed at the maximum speed at which the pilot felt he could maintain adequate control of the aircraft. The slalom course is a very useful tool for maneuver studies since it is repeatable and incorporates many maneuvers found in the other tasks.

Teardrop Turn

The teardrop turn illustrated in figure 4(b) involves passing over a point, rolling into a banked turn, and returning immediately to the same point. The maneuver is performed by rolling either right or left, holding the banked attitude, and then rolling back level before the aircraft passes back over the target.

S-Turn

The S-turn maneuver as shown in figure 4(c) is a side-step maneuver to avoid some obstacle. It involves a 90^{o} turn in one direction, leveling, and then another 90^{o} turn in the opposite direction to bring the aircraft parallel to the original flight path.

Hit-the-Deck

The hit-the-deck maneuver shown in figure 4(d) is used for rapid descents from an observation altitude or cruise altitude to an altitude behind cover. The maneuver involves a collective-pitch reduction and pitch-under. When the desired lower altitude is reached, power is increased and the helicopter continues in flight close to the ground.

Scramble

The scramble illustrated in figure 4(e) was performed both from a hover and from the ground. The scramble is used in nap-of-the-earth flying for rapid take-offs with the vehicle remaining close to the ground. The maneuver is performed by lifting off and simultaneously pitching forward, employing maximum power.

Whoa-Boy

The whoa-boy (fig. 4(f)) is a quick-stop maneuver consisting of a longitudinal and a lateral flare. The maneuver is performed by pitching slightly nose-up and making a rapid

90° yaw with a lateral flare. The maneuver is used in place of a longitudinal flare so that the helicopter may remain close to the ground during the flare.

RESULTS AND DISCUSSION

General Procedure

The results presented were obtained from the flight records for each type of maneuver described in the previous section. The measured bending moments and cyclic pitch are plotted as cyclic amplitudes about their mean values, based on readings about every 0.2 second, with care taken to include all peaks. The mean loads are not presented since they are not considered critical. The structural data are presented as bending moments, but in order to realize the practical significance of these moments, they may be converted to stresses by using the stress-conversion diagram in figure 5.

The coupled endurance limit, which is indicated on each bending-moment trace, is based on a representative flapwise cyclic bending-moment amplitude and the particular chordwise cyclic bending-moment amplitude required to exceed an assigned alternating stress limit of ±20 000 psi (±137 900 000 N/m^2) at a corner of the hub cross section (station 6). The maximum stress is dependent on the phasing of the two moments but, for simplification, it is considered conservative to assume that the moments are in phase, which is often the case. A summary of the tasks and the results to be discussed is presented in table II.

Slalom Course

400-ft (122-m) markers.- The pertinent data for the slalom course with 400-ft (122-m) spaced markers are plotted in figure 6. The parameters shown are the cyclic blade-angle amplitudes, aircraft pitching and rolling angular velocities, envelopes of the cyclic chordwise and flapwise bending-moment amplitudes, and the normal acceleration.

For the slalom run the helicopter is rolled left as it passes the first marker, right as it passes the second marker, and so forth. The initial right roll required to enter the slalom is not shown in figure 6.

Decreases in the cyclic pitch and in the cyclic chordwise and flapwise bending-moment amplitudes are noted as the helicopter builds up right rolling velocity. When the helicopter is rolling left, the cyclic pitch and the cyclic bending moments increase. During the left rolling maneuver the combined cyclic chordwise and flapwise bending moments give stresses well above the endurance limit of the hub.

The rise in chordwise and flapwise cyclic bending moments with left roll is at least partially due to the large increase in the cyclic pitch. The direct dependence of the cyclic bending moments on cyclic pitch is indicated in the equations of appendixes B and C of reference 3.

The asymmetrical behavior and lack of coordination of the test helicopter during the slalom maneuvers are functions of several complex aerodynamic and dynamic factors, some of which are inherent in all helicopters. These factors are listed in appendix A.

200-ft (61-m) markers.- Figure 7 shows that the results for the slalom course with the 200-foot (61-m) markers are similar to those shown in figure 6 for the course with 400-foot (122-m) markers. Although it is not readily apparent from figures 6 and 7, an examination of all the data runs shows that the loadings resulting from the slalom course with 200-foot (61-m) markers were generally more severe than those from the slaloms with 400-foot (122-m) markers. The trend of higher cyclic bending moments in left roll is again apparent in figure 7.

A detailed time history of a roll reversal from another 200-foot (61-m) marker slalom run is shown in figure 8. This figure shows the actual cyclic variations of bending moments as functions of the azimuth angle rather than a time history of maximum amplitudes as shown in figures 6 and 7. Again the difference between the left and right roll is apparent. This particular roll reversal was the most severe loading condition encountered during this investigation. The maximum flapwise cyclic bending moment was nearly ±20 000 in-lb (±2260 N-m) and the maximum chordwise cyclic bending moment was over ±160 000 in-lb (±18 100 N-m) which, added directly, gave a maximum cyclic stress of ±60 000 psi (±413 682 000 N/m^2). This high stress level would be acceptable statically, but when applied as an alternating stress it results in rapid deterioration of the service life of the rotor hub. Considering that the slalom course, as well as the nap-of-the-earth maneuvers it was devised to simulate, consists of a series of roll reversals, the fatigue of the rotor components could result in serious limitations of the maneuver capability of the hingeless-rotor helicopter. It is also to be noted in figure 8 that drastic fluctuations occur in the normal acceleration during the left roll. These fluctuations led to bottoming of the spring-mounted cabin and to large fluctuations in the cyclic bending moments (primarily chordwise). The normal-acceleration fluctuations are related to the lack of coordination during the slalom maneuvers. (See appendix A.)

A more closely coordinated (smoother) slalom came about after the pilot had a significant amount of experience in coping with the inherent problems of the helicopter.

A detailed time history of a roll reversal from a more closely coordinated slalom is shown in figure 9. It can be seen that the magnitudes of the fluctuations in normal acceleration and cyclic bending moments are substantially reduced; however, the resulting stresses are still well above the assigned endurance limit.

The buildup in cyclic bending moments during roll reversals of hingeless rotors is also evident in figure 10, which shows a detailed time history of a roll reversal performed in a rudimentary hingeless-rotor helicopter, the XH-13N. (See refs. 2 and 3.)

By referring again to figures 8 and 9, it can be seen that the flapwise bending-moment trace of the XH-51N shows the effects of extensive random loadings. This random loading is tentatively ascribed to nonharmonic feedback from the blades to the control gyro when the blades strike the tip vortex of the preceding blades and to the coupling of the controls with the vertical motion of the spring-mounted cabin, as mentioned in appendix A. The vertical motion of the cabin is aggravated by excessive collective stick sensitivity. The XH-13N did not employ a control gyro or spring-mounted cabin, and the flapwise bending-moment trace in figure 10 is seen to be relatively free of nonharmonic loadings.

Teardrop Turn and S-Turn

Figure 11 shows the time history of one teardrop turn. The maneuver was performed at an entry speed of 70 knots and again, during the left roll, there is a rapid buildup in the rotor-hub cyclic bending moments. Figure 12 shows the time history of an S-turn performed at an entry speed of 65 knots. As in the other maneuvers requiring roll-control inputs, stresses are fairly severe during the left roll and there is a rapid buildup in the cyclic bending moments.

Hit-the-Deck and Scramble From the Ground

The pitching maneuvers of the hit-the-deck and scramble shown in figures 13 and 14, respectively, were far less severe than the rolling maneuvers. Again, as expected, the bending-moment traces follow the cyclic pitch.

Whoa-Boy

The whoa-boy maneuver shown in figure 15 is the least severe of the six maneuvers from the standpoint of chordwise dynamic loading. However, the flapwise cyclic moments maintain a fairly high level throughout the maneuver.

Methods of Alleviating the High Cyclic Hub Moments During Nap-of-the-Earth Maneuvers

During this investigation the control gyro of the XH-51N was lightly damped. An increase in the mechanical damping on the gyro, the elimination of the coupling between control inputs and cabin motion, and the reduction of the collective sensitivity may result in the reduction of the chordwise and flapwise stresses during maneuvers. Other possibilities for reducing the maneuver loads include variable tail incidence in order to induce

a favorable change in the required cyclic pitch and reduced in-plane stiffness to allow more centrifugal relief of the chordwise moments (refs. 2, 3, and 5).

SUMMARY OF RESULTS

Results of this brief investigation of the rotor-hub cyclic bending moments of a hingeless-rotor helicopter during nap-of-the-earth maneuvers may be summarized as follows:

1. The rotor-hub cyclic bending moments were severe, especially during rapid roll reversals, and require specific design attention (possibly a different design approach) to avoid limiting the maneuver capability of a hingeless-rotor helicopter.

2. The test helicopter behaved asymmetrically between right and left roll, and the resulting stresses were substantially higher during the left rolls than during the right rolls.

3. The degree of coordination which the pilot was able to achieve during the maneuvers had a substantial effect on the cyclic bending moments.

4. An operational aircraft with a hingeless rotor will require careful evaluation during nap-of-the-earth flying in order to establish the overall service life of the rotor system.

Langley Research Center,
National Aeronautics and Space Administration,
Langley Station, Hampton, Va., January 24, 1968,
721-02-00-02-23.

APPENDIX A

FACTORS RELATING TO ASYMMETRICAL BEHAVIOR OF TEST HELICOPTER AND LACK OF COORDINATION DURING SLALOM MANEUVERS

The flight data and pilot comment have revealed that rapid negotiation of the slalom course in the test helicopter results in asymmetrical behavior and difficulties in coordination. Some of the factors relating to these findings are as follows:

1. Longitudinal inflow variation and coning in forward flight which results in lateral aircraft moments (lateral trim shift). (This factor is inherent to some extent in all types of rotors.)

2. Fuselage and rotor-pylon interference may be occurring in the azimuth positions aft of the rotor pylon. (This factor could be inherent to some extent in all helicopters but may be larger in a helicopter where the rotor is mounted close to the fuselage.)

3. Excessive collective-pitch sensitivity which leads to poor power coordination and high fluctuations in normal acceleration (0.4g to 0.6g per in. (0.15g to 0.23g per cm) of collective stick).

4. Control inputs couple with vertical motion of the spring-mounted cabin (0.83 in. (2.11 cm) of longitudinal control per g and 0.50 in. (1.27 cm) of lateral control per g).

5. Asymmetric adverse yaw which leads to poor directional control.

6. Crosswinds which cause alternating upwind and downwind turns.

7. Cross-coupling of rotor pitch and roll control inputs which results from gyro-control springs acting through bellcrank motions which become nonlinear for large pilot control inputs.

The combination of all or some of these factors results in an erratic and poorly coordinated maneuver and subsequently in high blade stresses.

The NASA research pilot who performed the flights reported in this paper has subsequently flown an uninstrumented production-prototype version of the test helicopter through the slalom course. This prototype, which had several modifications including rigid mounting of the cabin, appeared to perform the maneuvers in a smoother and more coordinated manner.

APPENDIX B

INSTRUMENTATION

Main Rotor:

Strain gages:

- Hub flapwise bending at a station 6 in. (15.2 cm) from center line of main rotor
- Hub chordwise bending at a station 6 in. (15.2 cm) from center line of main rotor
- Mast bending 90^{o} from instrumented hub arm
- Mast bending 0^{o} from instrumented hub arm
- Axial-load pitch link

Position transmitters:

- Blade angle

Control System:

Strain gages:

- Axial load of boost-idler linkages, longitudinal and lateral
- Axial load of swash-plate linkages, longitudinal and lateral
- Control-stick force, longitudinal and lateral

Position transmitters:

- Swash plate, longitudinal and lateral positions
- Control stick, longitudinal and lateral positions

Accelerations and Angular Velocities:

Rate gyros:

- Pitch rate in transmission compartment
- Roll rate in cabin

Accelerometers:

- Longitudinal, lateral, and vertical cabin accelerations

APPENDIX B

Vibrations:

Vibration pickups:

Longitudinal, lateral, and vertical cabin vibrations
Longitudinal, lateral, and vertical transmission vibrations

Horizontal Tail:

Vertical bending at a station 9 in. (22.8 cm) from center line of fuselage

Tail Rotor:

Strain gages:

Flapwise bending at a station 19.5 in. (49.5 cm) from center line of tail rotor
Chordwise bending at a station 19.5 in. (49.5 cm) from center line of tail rotor
Axial loads in pitch link

Performance:

Airspeed
Altitude
Engine and fuel-control parameters

REFERENCES

1. Huston, Robert J. (with appendix A by Robert J. Huston and William J. Snyder): An Exploratory Investigation of Factors Affecting the Handling Qualities of a Rudimentary Hingeless Rotor Helicopter. NASA TN D-3418, 1966.

2. Huston, Robert J.; and Ward, John F.: Handling Qualities and Structural Characteristics of the Hingeless-Rotor Helicopter. Conference on V/STOL and STOL Aircraft, NASA SP-116, 1966, pp. 1-16.

3. Ward, John F.: Exploratory Flight Investigation and Analysis of Structural Loads Encountered by a Helicopter Hingeless Rotor System. NASA TN D-3676, 1966.

4. Wyrick, D. R.; and Buzzetti, C. J.: Final Flight Test Report and Pre-Military Research Evaluation Conference Report – XH-51A Rigid Rotor Helicopter. Rept. No. 16933 Suppl. I (Contract No. NOw 62-0665-d), Lockheed-California Co., Sept. 10, 1963.

5. Lockheed-California Co.: Investigation of Elastic Coupling Phenomena of High Speed Rigid Rotor Systems. TRECOM Tech. Rept. 63-75 (Lockheed Rept. No. 17013), U.S. Army Transportation Res. Command (Fort Eustis, Va.), June 1964.

6. Burpo, Frank B.: Maneuverability Data From an Army Helicopter Flying a Simulated Armament Mission. Rept. No. 831-099-003, Bell Helicopter Co., Apr. 1965.

TABLE I.- PHYSICAL PARAMETERS OF XH-51N

Main rotor (hingeless):	
Number of main-rotor blades	3
Main-rotor diameter	35 ft (10.7 m)
Main-rotor blade chord	13.5 in. (34.3 cm)
Main-rotor disk area	962 ft^2 (89.4 m^2)
Solidity	0.0614
Airfoil section	NACA 0012
Blade twist (linear washout)	-5^o
Fixed coning angle, hub	2.8^o from horizontal
Fixed coning angle, blade	1.8^o from horizontal
Normal rotor speed	355 rpm
Blade weight	86 lbf/blade (382 N/blade)
Rotor mass moment of inertia	760 slug-ft^2 (1030 kg-m^2)
Blade sweepforward at 75 percent radius	2.25 in. (5.7 cm)
Flapwise natural frequency of rotating blade	40.9 rad/sec
Chordwise natural frequency of rotating blade	52.3 rad/sec
Control gyro:	
Diameter	77 in. (196 cm)
Gyro mass moment of inertia	7.5 slug-ft^2 (10.2 kg-m^2)
Tail rotor (teetering):	
Number of blades	2
Rotor diameter	6 ft (1.83 m)
Disk area	28.27 ft^2 (2.63 m^2)
Blade chord	8.5 in. (21.6 cm)
Solidity	0.149
Airfoil section	NACA 0012
Blade twist	-4.40^o
Fixed coning angle	0^o
Normal rotor speed	2085 rpm
Rotor mass moment of inertia	0.302 slug-ft^2 (0.41 kg-m^2)
Effective cant angle of flapping hinge	15^o
Horizontal tail:	
Span	84 in. (2.13 m)
Chord	13 in. (33 cm)
Area	7.55 ft^2 (0.7 m^2)
Aspect ratio	6.45
Fixed incidence angle	-5.5^o
Airfoil section	NACA 0015
Gross weight for this investigation (right seat, pilot; left seat, lead ballast)	4100 lbf (18 238 N)
Longitudinal center of gravity for this investigation, from center line of main rotor	0.3 in. (0.8 cm) aft
Lateral center of gravity for this investigation, from center line of main rotor	0 in. (0 cm)

TABLE II.- SUMMARY OF TASKS AND RESULTS

Task	Predominant maneuvers	Approximate time to complete task, sec	Percent of time spent above assigned endurance limit	Comments
Slalom course	Rapid roll reversals	30	40	Stresses occur far in excess of assigned endurance limit
Teardrop turns	Rolling and pitching	20	50	Moderately high stresses
S-turn	Rolling	16	30	Moderately high stresses
Hit-the-deck	Pitching	8	18	Moderate stresses
Scramble	Pitching	10	40	Moderate stresses
Whoa-boy	Pitch, yaw, and roll	10	30	Moderate stresses

Figure 1.- Experimental hingeless-rotor helicopter XH-51N.

L-68-839

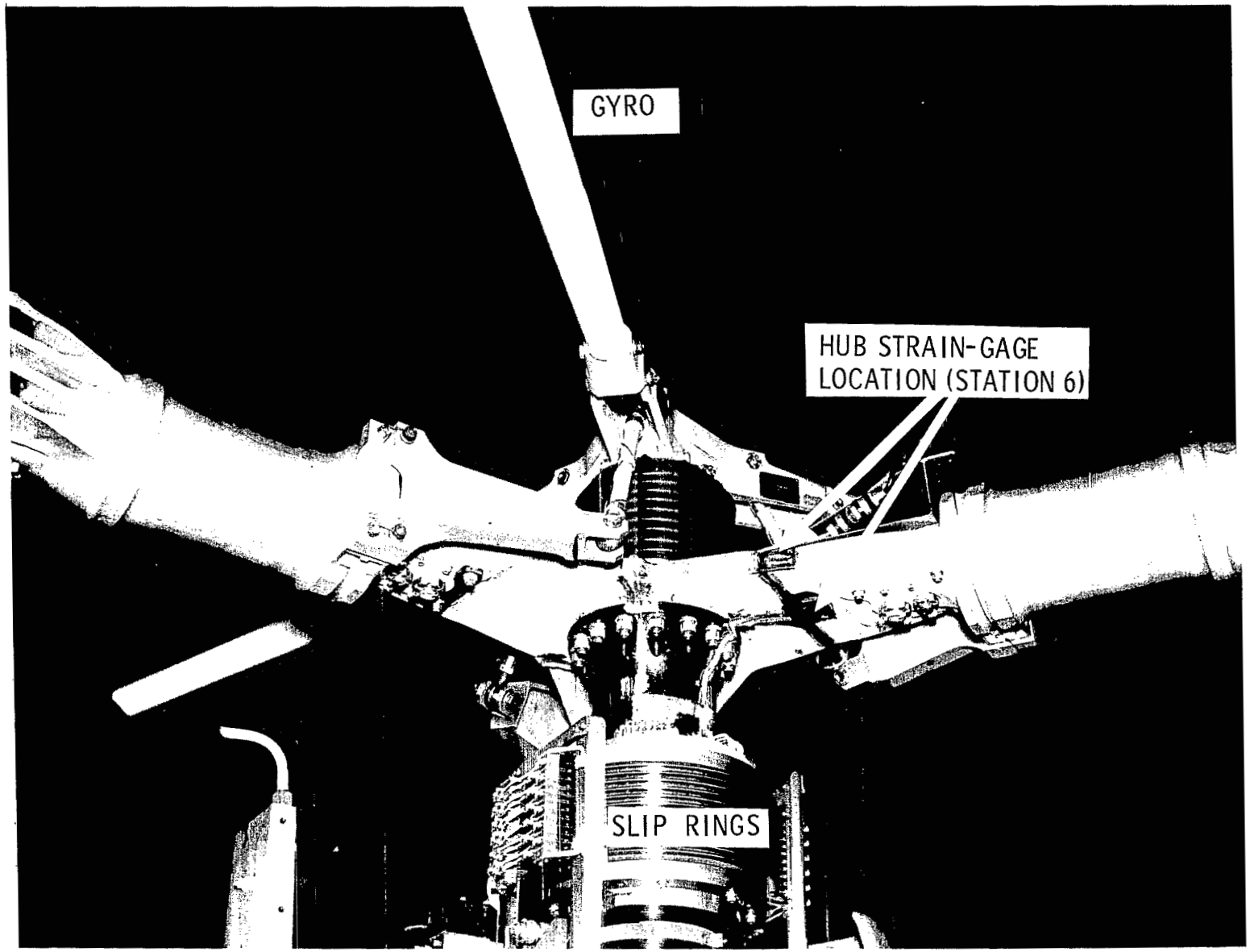

Figure 2.- Photograph of XH-51N hub and mast showing locations of strain gages.

L-68-840

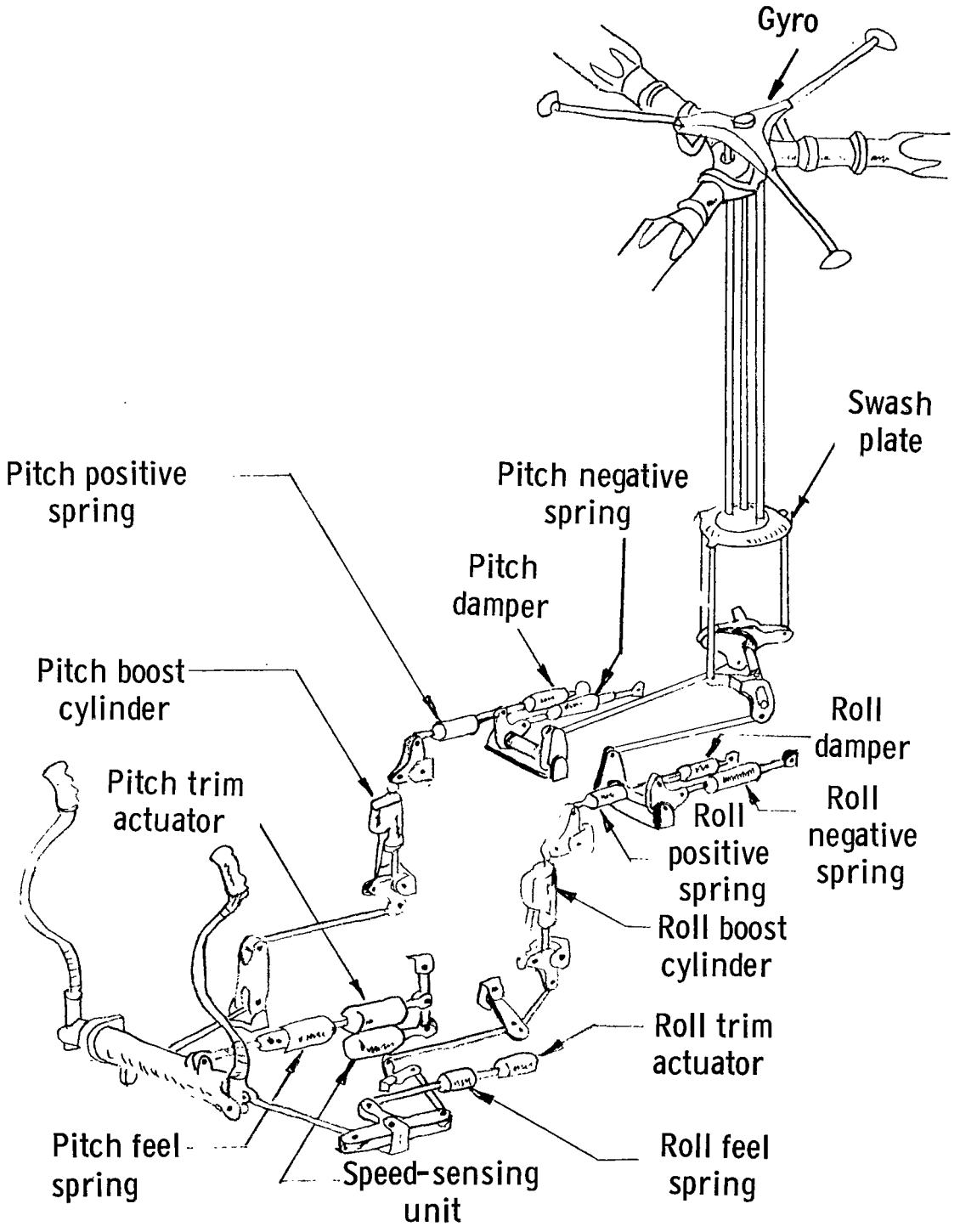

Figure 3.- Control-system details of XH-51N helicopter.

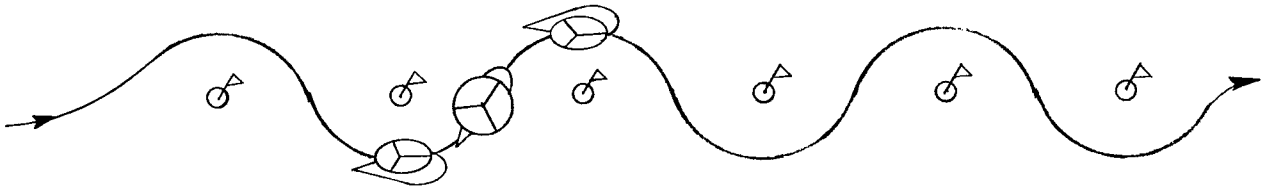

(a) Slalom course (top view).

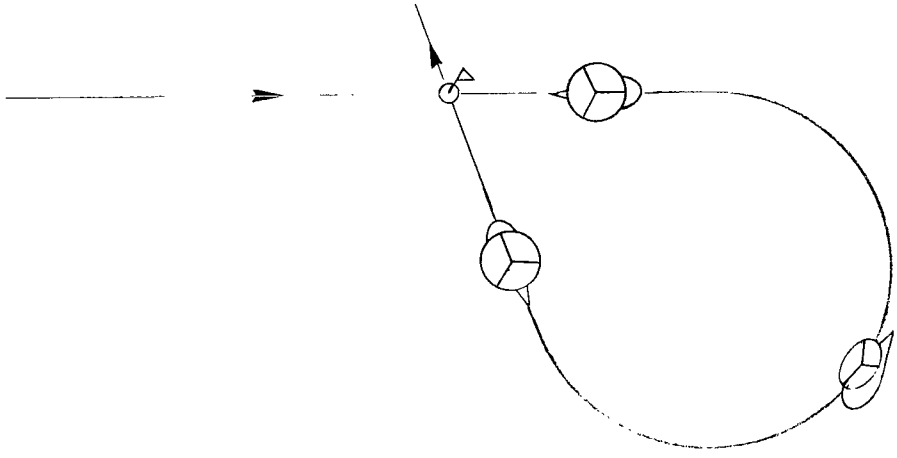

(b) Teardrop turn (top view).

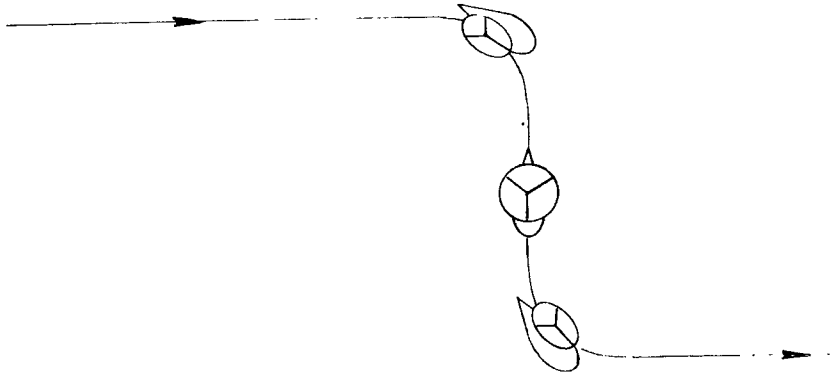

(c) S-turn (top view).

Figure 4.- Maneuver tasks.

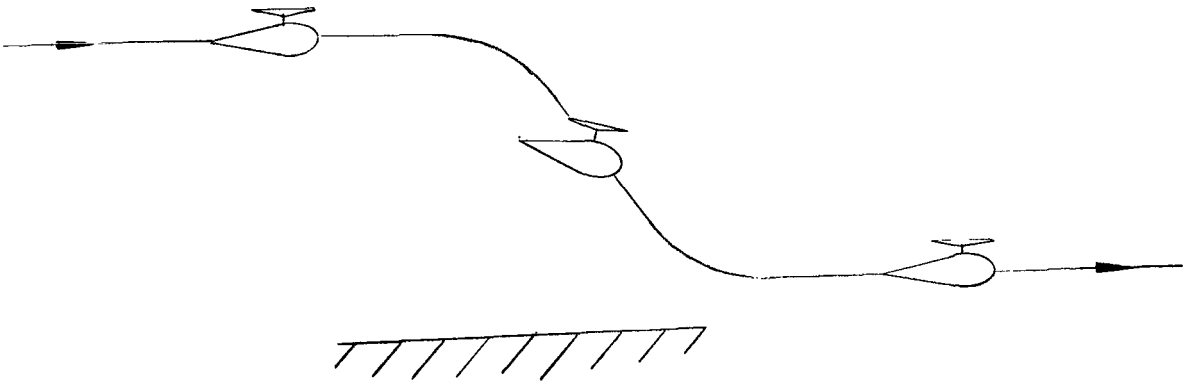

(d) Hit-the-deck (side view).

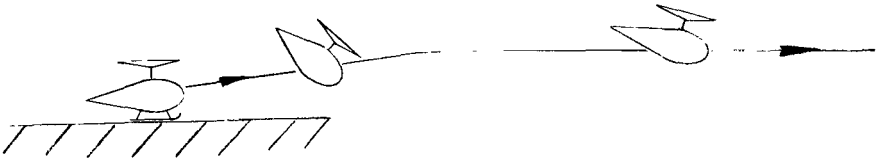

(e) Scramble (side view).

(f) Whoa-boy (side view).

Figure 4.- Concluded.

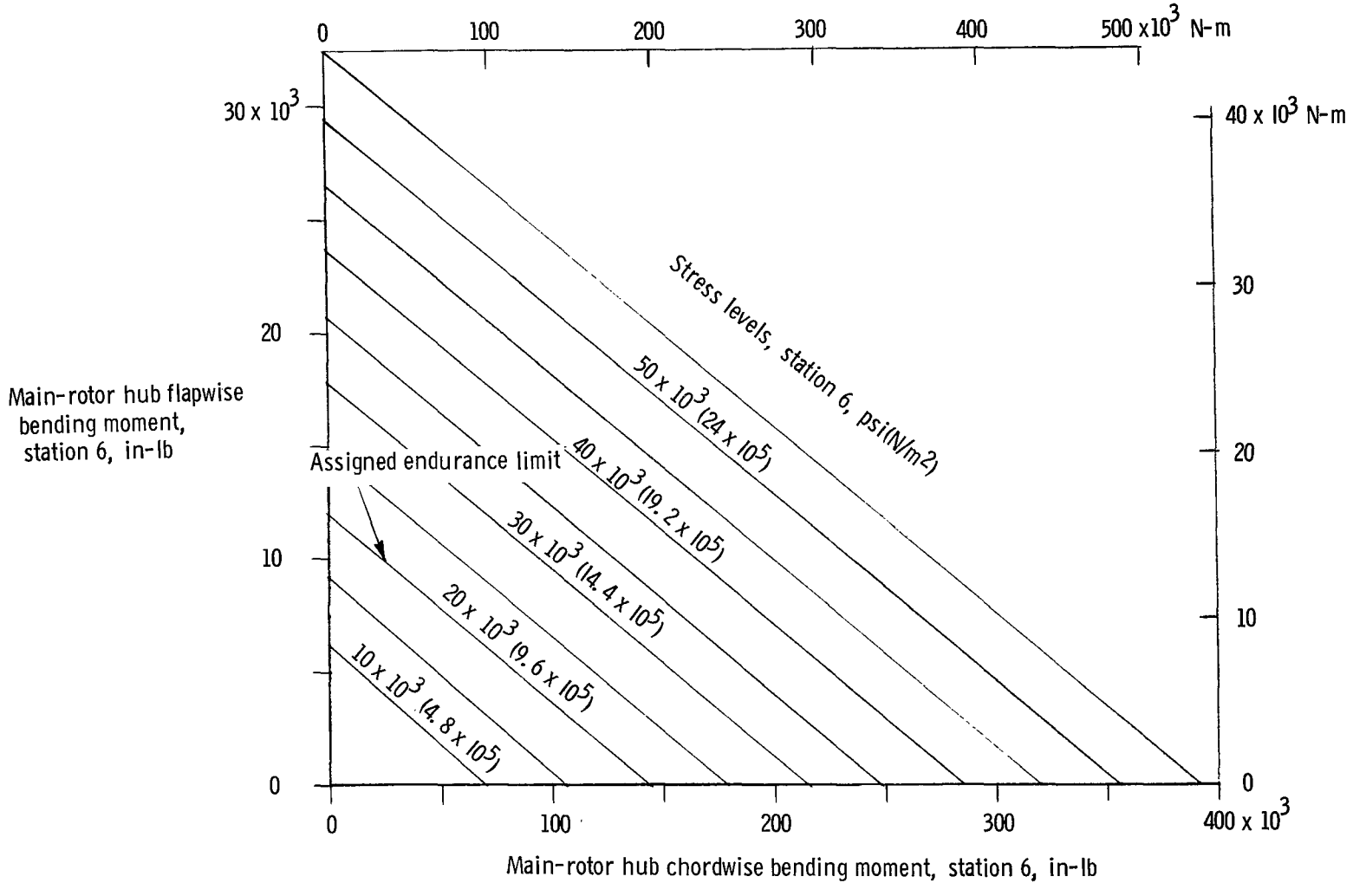

Figure 5.- Conversion diagram for determining maximum stresses from chordwise and flapwise bending moments.

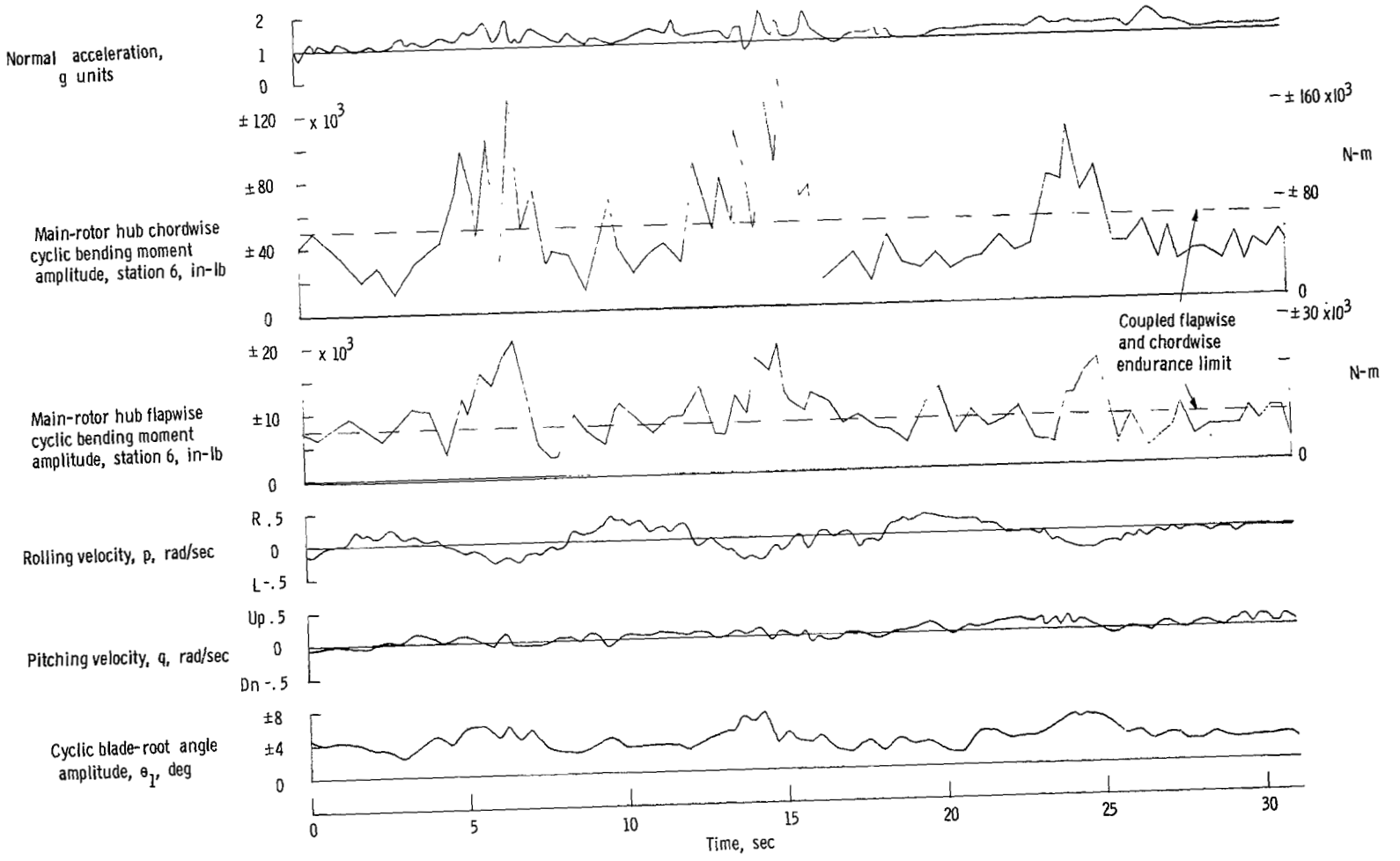

Figure 6.- Slalom-course maneuver performed at 70 knots through 400-foot (122-m) spaced markers.

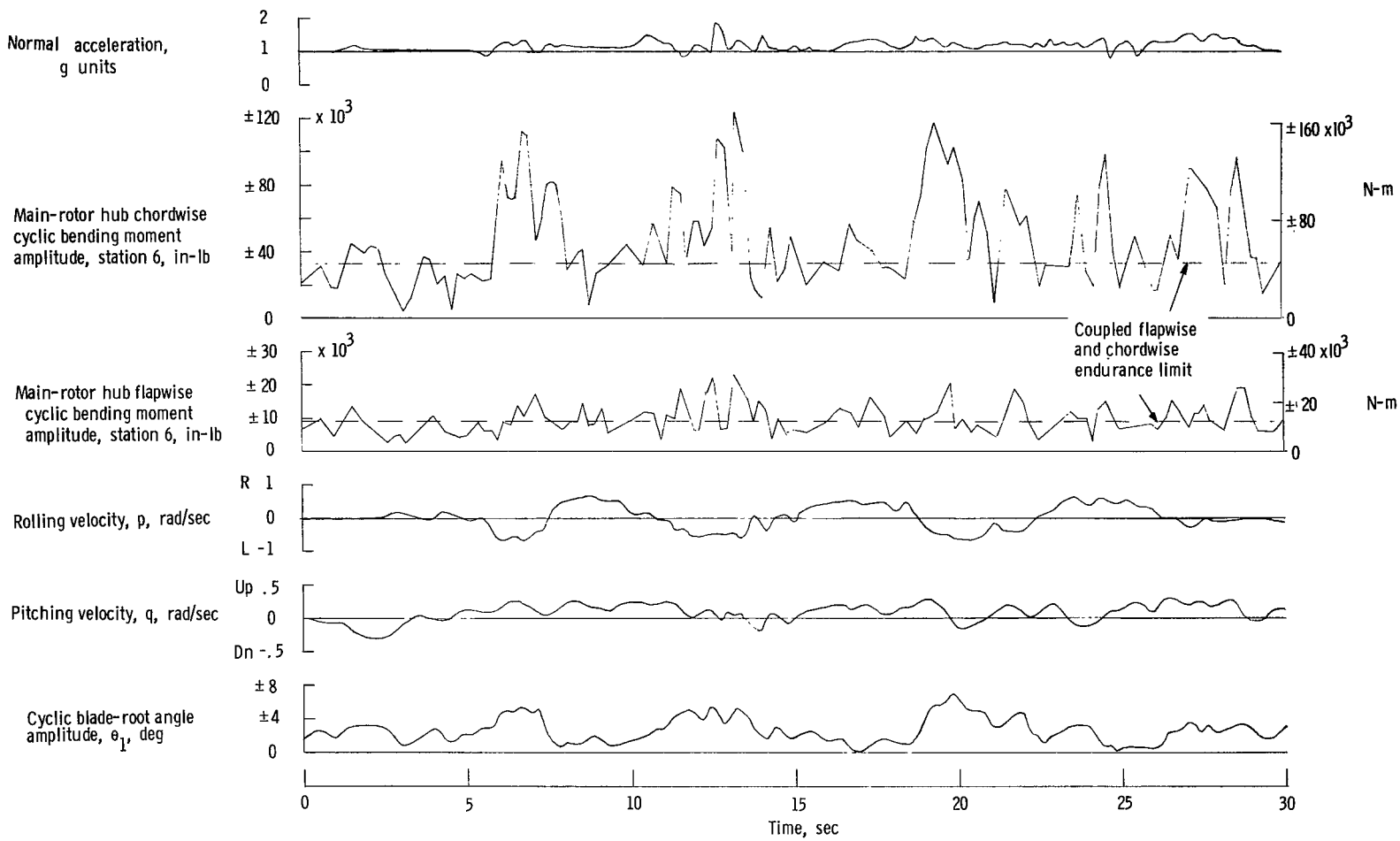

Figure 7.- Slalom-course maneuver performed at 45 to 50 knots through 200-foot (61-m) spaced markers.

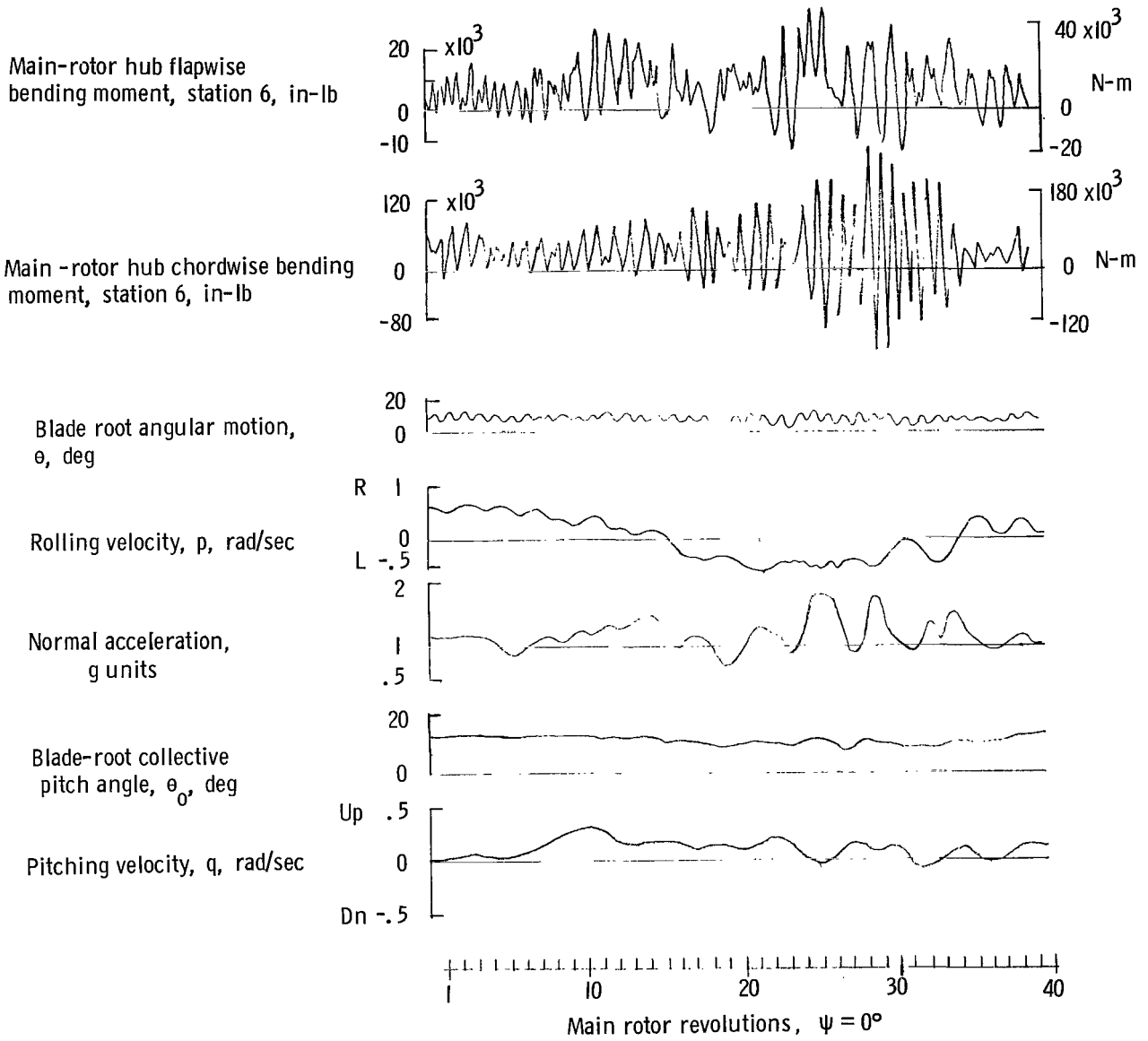

Figure 8.- Roll reversal performed at 45 to 50 knots during negotiation of early slalom course with 200-foot (61-m) markers in the XH-51N.

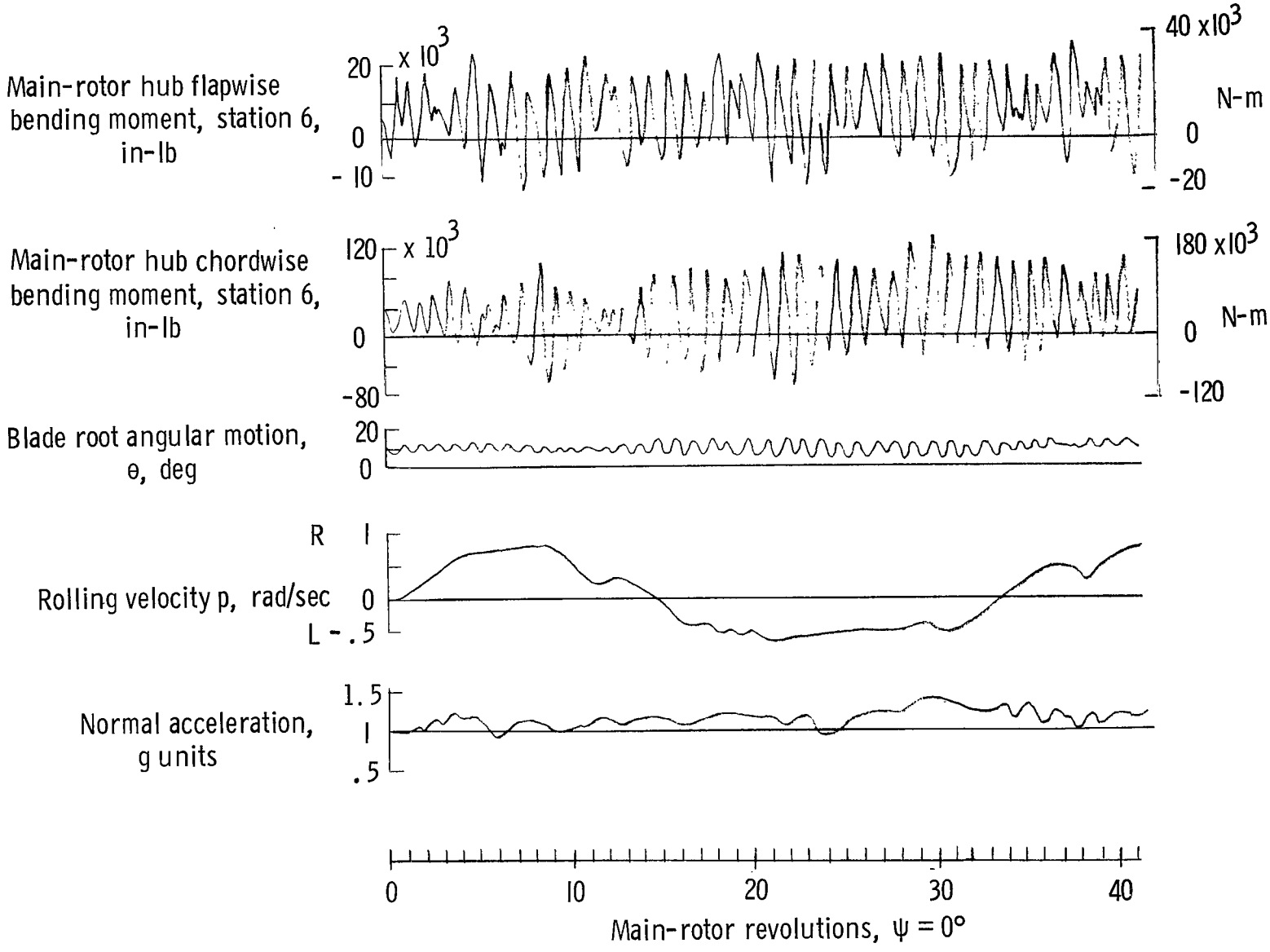

Figure 9.- Roll reversal performed at 45 knots during negotiation of last slalom course with 200-foot (61-m) markers in the XH-51N.

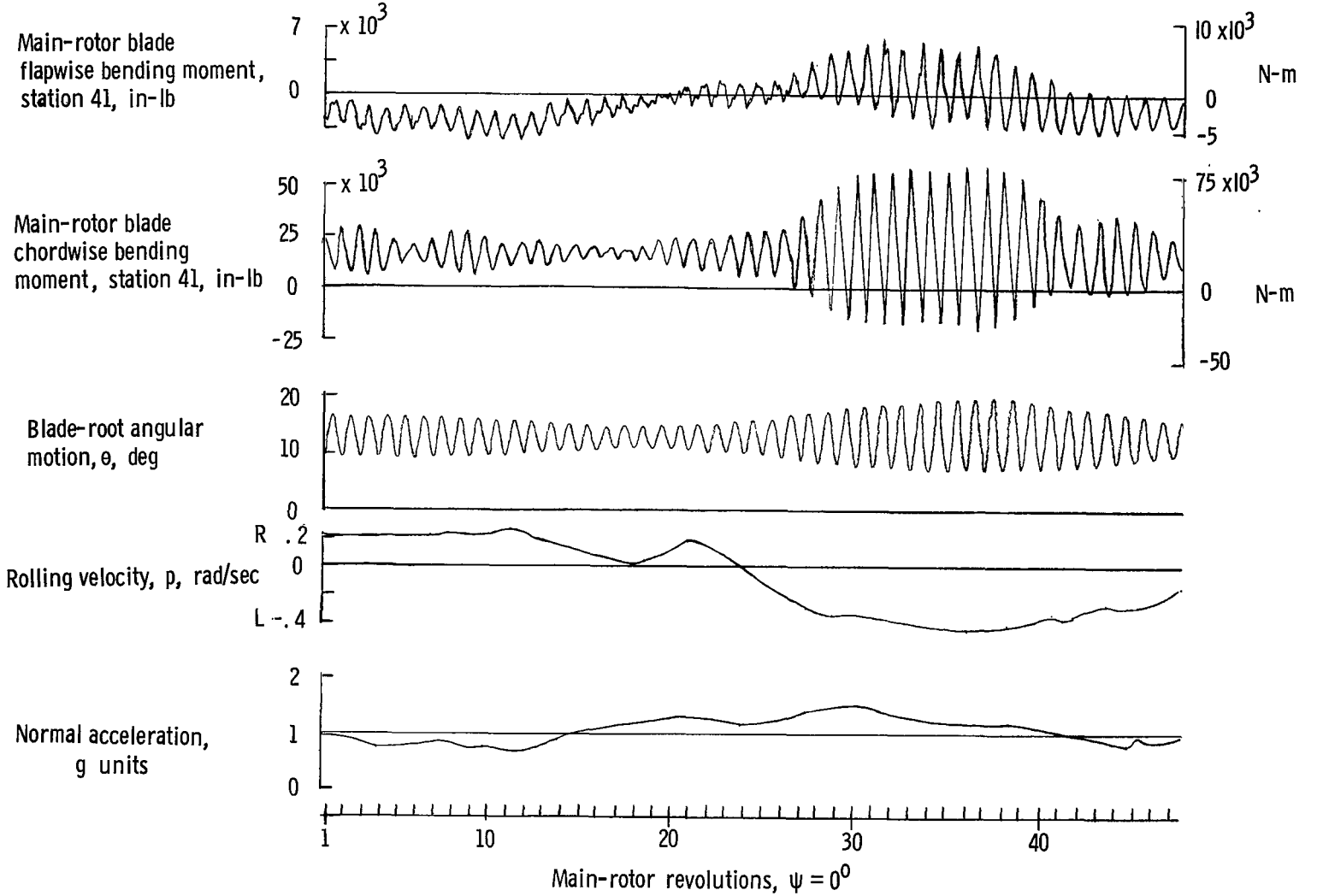

Figure 10.- Roll reversal performed at 70 knots in XH-13N.

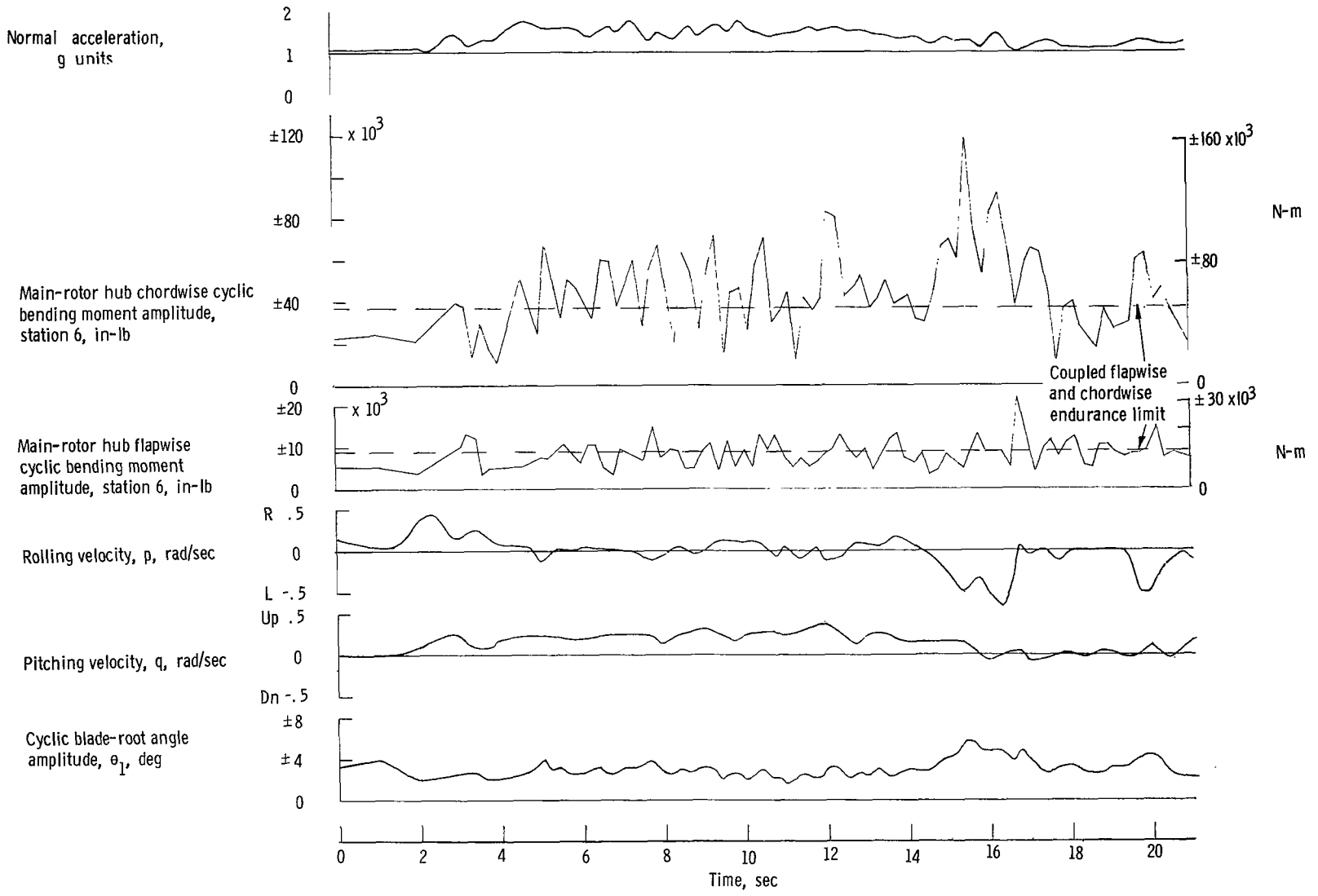

Figure 11.- Teardrop turn performed at an entry speed of 70 knots.

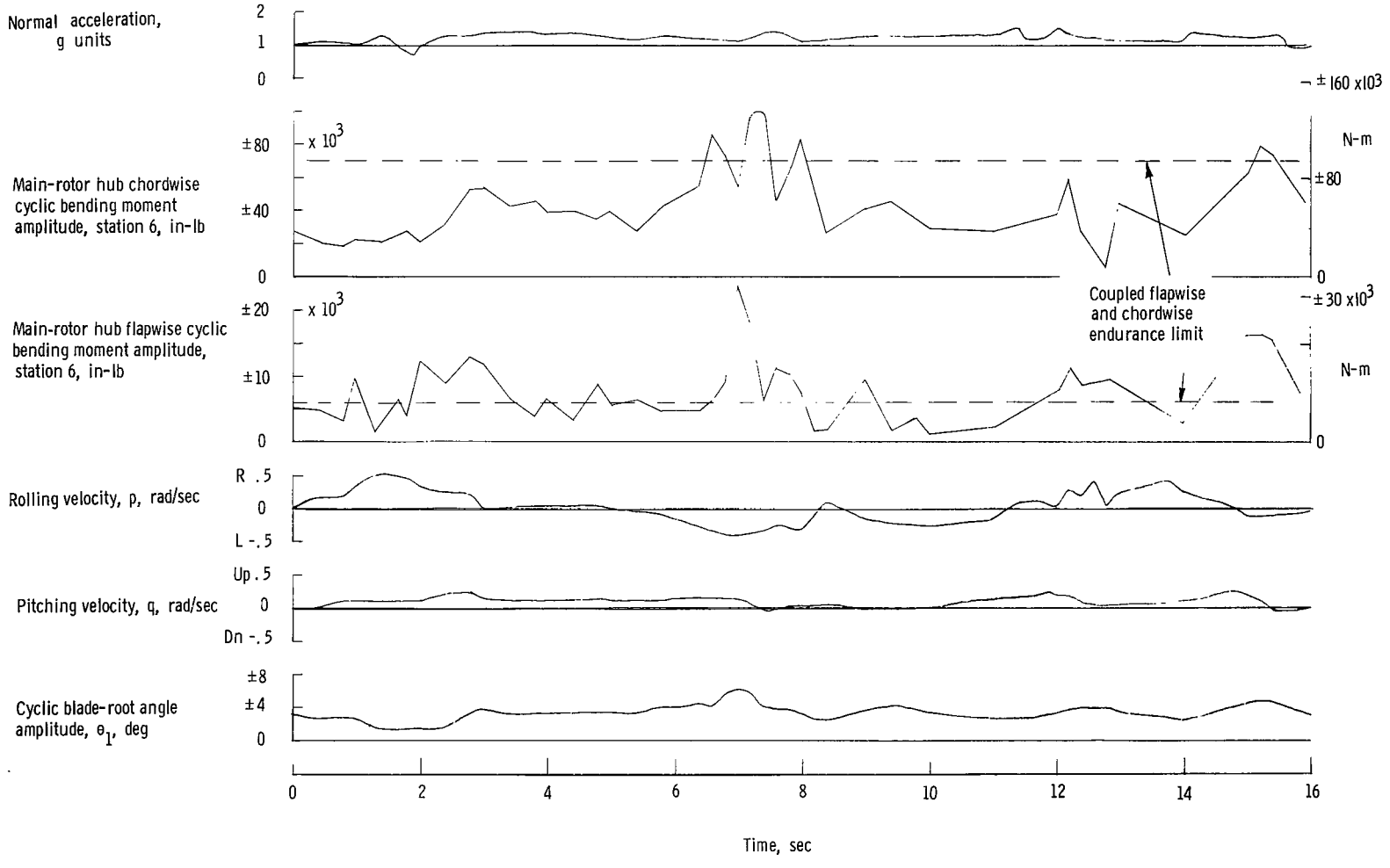

Figure 12.- S-turn performed at an entry speed of 65 knots.

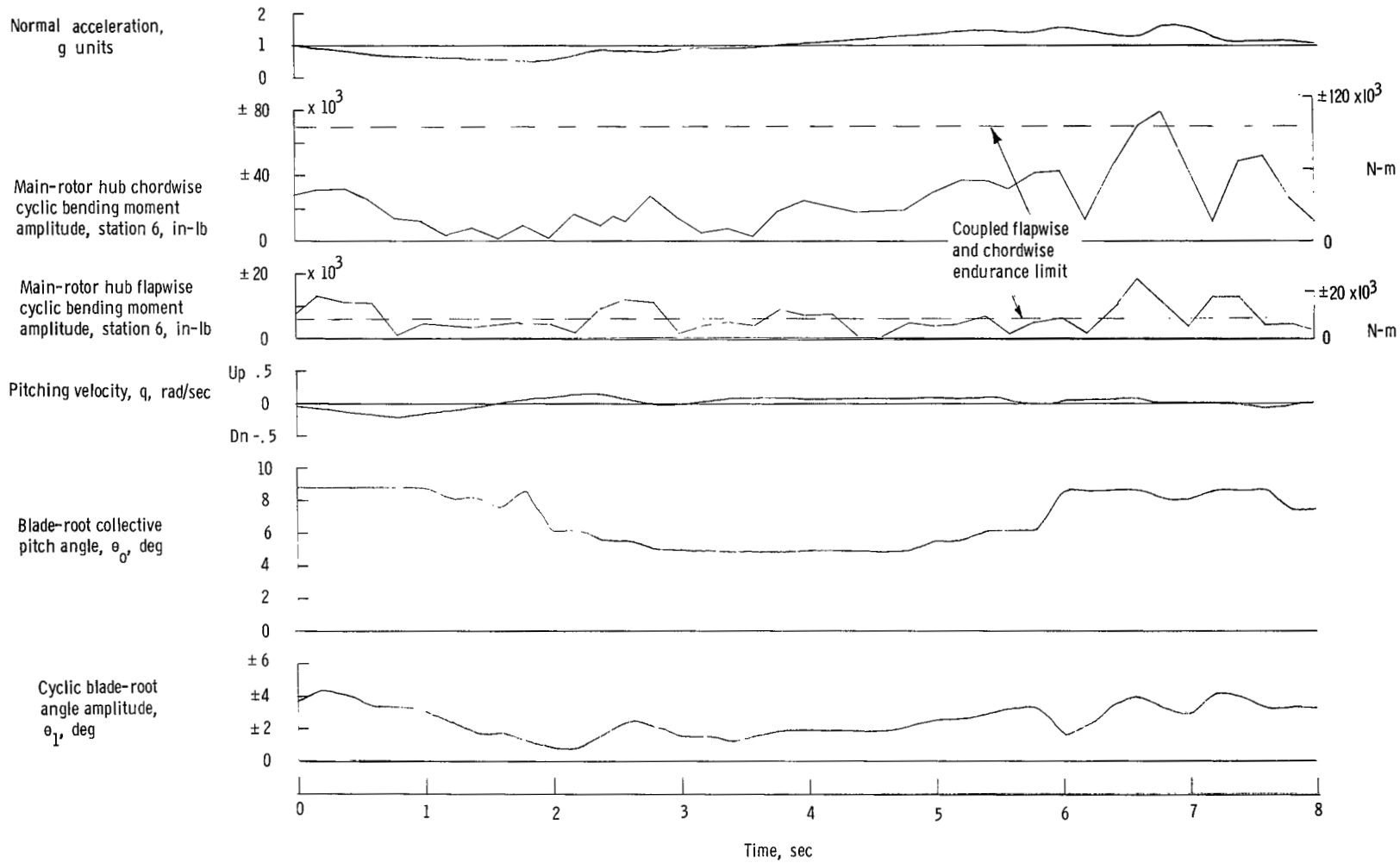

Figure 13.- Hit-the-deck maneuver from 200-foot (61-m) altitude with entry speed of 70 knots.

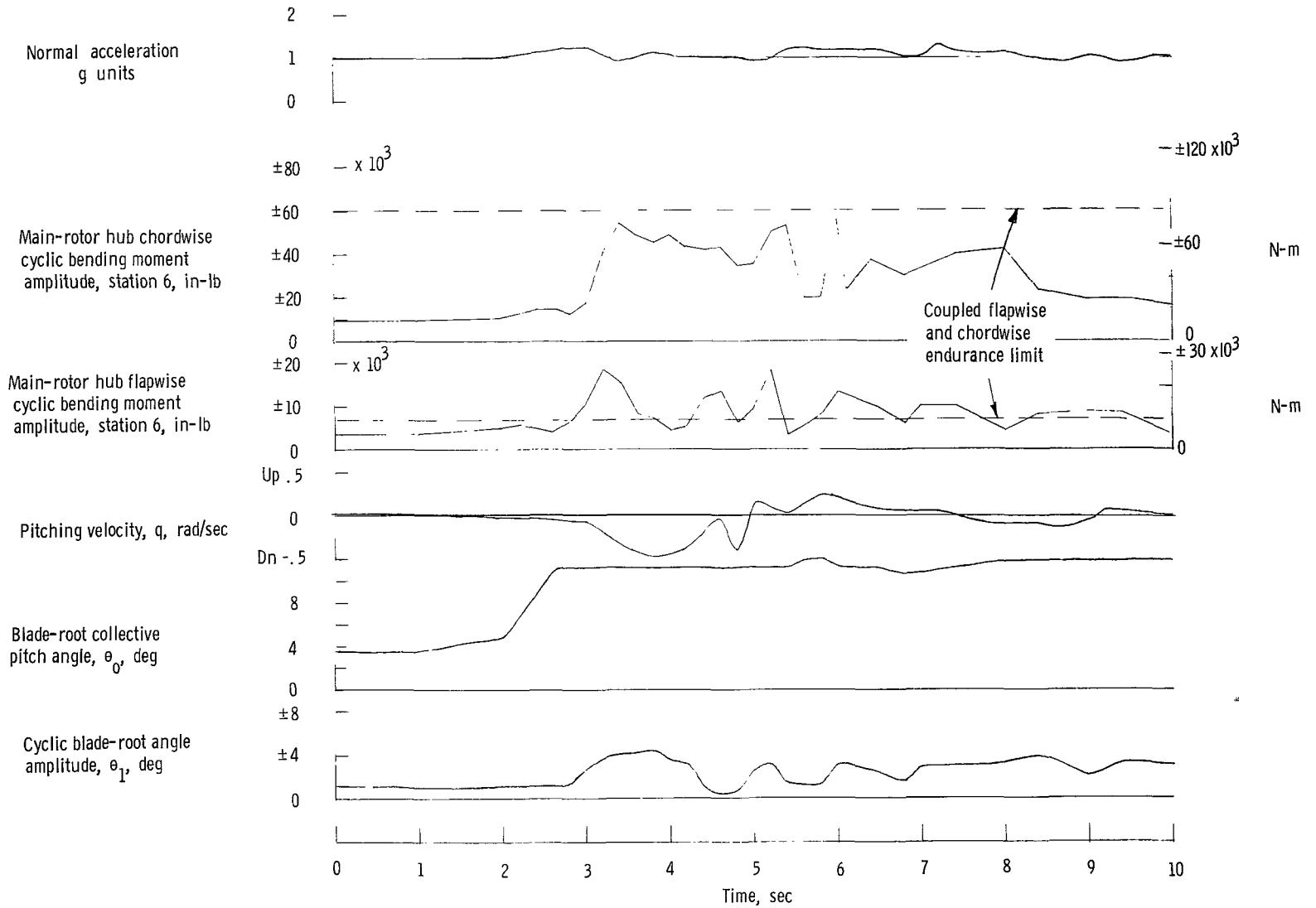

Figure 14.- Scramble maneuver from ground to 80 knots.

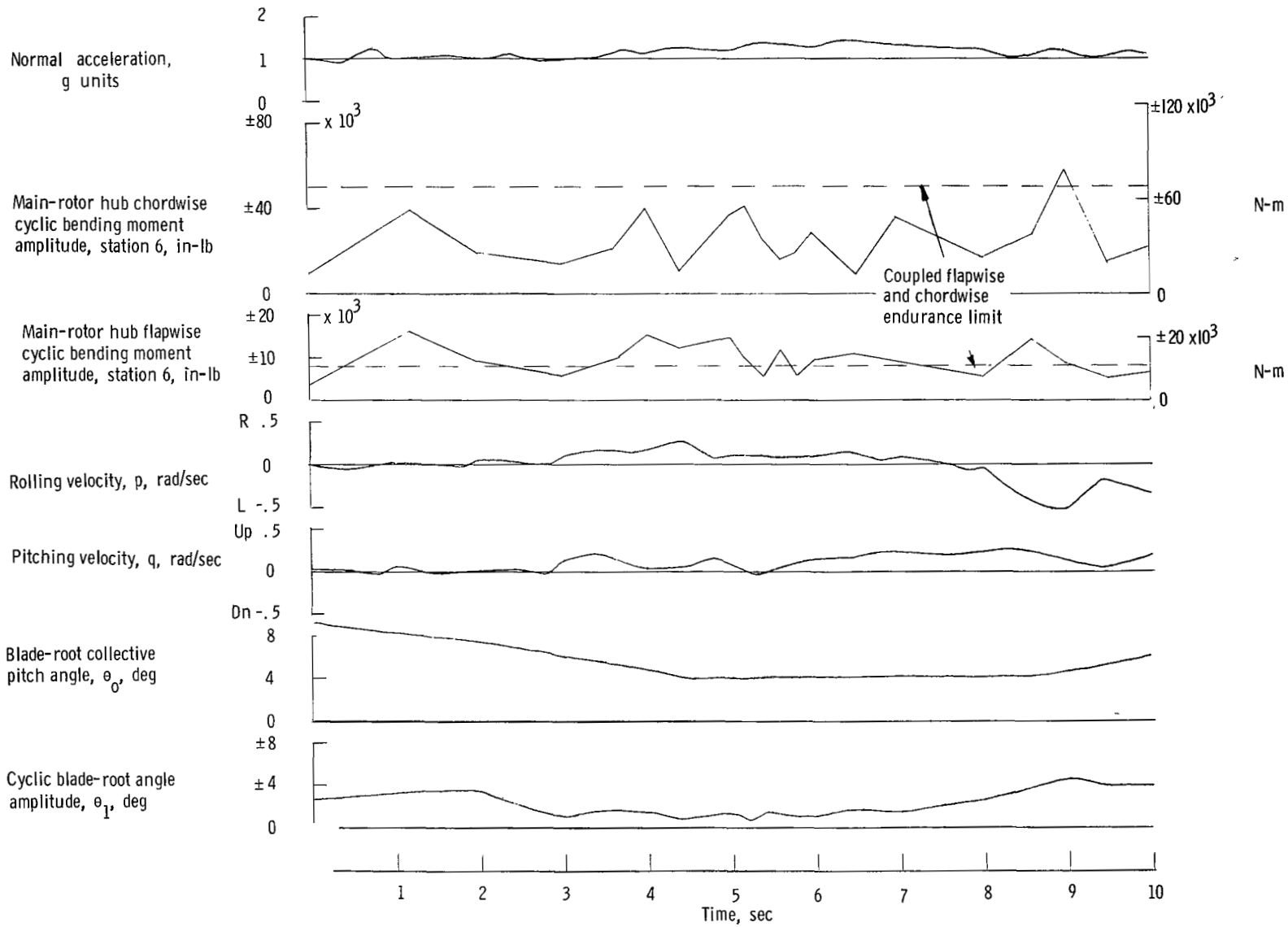

Figure 15.- Whoa-boy maneuver with entry speed of about 80 knots.